Pergamon

Int. J. Heat Mass Transfer. Vol. 38, No. 5, pp. 795–805, 1995

0017–9310/95 $9.50+0.00

0017–9310(94)00214–2

Direct-contact condensation in the presence of noncondensables over free-falling films with intermittent liquid feed

T. D. KARAPANTSIOS and A. J. KARABELAS†

Chemical Process Engineering Research Institute and Department of Chemical Engineering, Aristotle University of Thessaloniki, University Box 455, GR 540 06 Thessaloniki, Greece

(*First received* 15 *November* 1993 *and in final form* 16 *July* 1994)

Abstract—An intermittent (periodic) liquid flow rate is examined as a means to enhance local condensation rates in a vertical column where quasi-stagnant vapor–gas mixtures come in direct contact with falling wavy liquid layers. The gas mixture being effectively stagnant is responsible for the major resistance to heat transfer due to its relatively large concentration of noncondensables. Flow intermittency is found to improve heat transfer rates by as much as an order of magnitude. The local condensation heat transfer coefficients depend greatly on both liquid flow mode and liquid flow rate. For the range of frequencies encountered here, the flow cycling frequency seems to have only a minor effect on the transport process, whereas the asymmetry in the intermittency (flow/pause time periods) appears to be more significant. Statistical analysis of the measured local fluctuations of film thickness reveals that condensation is responsible only for slight modifications of the isothermal liquid surface morphology. There is also evidence that the interfacial transport process is aided by increased liquid wave velocities.

INTRODUCTION

Film condensation heat transfer inside vertical tubes has been the subject of intensive theoretical and experimental investigation for several decades. Considerable efforts have been made all these years to improve convective heat transfer in condensation equipment by various means. A comprehensive account on such methods is given by Collier [1] where classification is made into the following three categories:

(a) Application of non-uniform distribution of the fluid velocities with simultaneous increase of interfacial area; this is achieved by particular spatial geometric structures along the condensing surface, e.g. corrugated walls, adjunction of metallic grids or wires.

(b) Promotion of drop-wise rather than film wise condensation upon the surface; this is done by coating the surface with either a chemical or polymer or noble metal thin film ($< \sim 1$ μm) to render it non-wetting so that vapors may condense in a drop-wise manner.

(c) Use of force fields; centrifugal, electrostatic and vibrational external forces are applied to reduce condensate thickness and promote drainage.

Collier [1] reports that corrugated surfaces improve the condensation coefficients by several times (compared to plain tubes) at a low construction and maintenance cost. On the other hand, coatings suffer from aging and peeling problems while external force fields are criticized for the additional equipment and operational cost. So far, fluting the tube appears to be the most effective way to enhance condensation heat transfer.

There is sufficient evidence in the literature that the presence of waves on films, can cause a dramatic increase in transfer rates of heat (e.g. refs. [2, 3]) and mass (e.g. refs. [4, 5]) even for laminar flows. However, researchers have not reached a consensus yet on whether large (e.g. ref. [6]) or small (e.g. ref. [7]) waves control the interfacial transport processes. Investigations on the influence of interfacial waves of controlled frequency and amplitude (imposed by external means) over *horizontal* stationary liquid layers [8, 9] showed increases in mass transfer rates by more than an order of magnitude as compared to smooth films. However, superimposed vibrations to an already-rippled inclined film [4] appeared to damp out the natural roll waves of the surface, producing artificial sinusoidal undulations which had very little effect on mass transfer. In summary, there is not enough evidence in the literature on the kind of externally induced waves that may drastically alter interfacial transport.

The possibility of imposing a periodic (intermittent) fluid feed as a means to improve mass and heat transfer has received little attention. Brauner and Maron [10] discuss a droplet-type intermittent liquid feed in a horizontal-type evaporator–condenser. Improved transport rates were measured but the effect of this feed mode was observed to fade rapidly with distance from drop impingement position and to be largely dependent on dripping characteristics, drainage rate

†Author to whom correspondence should be addressed.

NOMENCLATURE

C_p	specific heat, [J kg^{-1} K^{-1}]
D	tube diameter [m]
h	condensation heat transfer coefficient, [J m^{-2} s^{-1} K^{-1}]
m_{con}	condensation rate [kg s^{-1}]
Re	liquid Reynolds number, $4\Gamma\,\mu^{-1}$, dimensionless
s	standard deviation
T	temperature [K]
t	time [s]
V_{wave}	average streamwise wave velocity, [m s^{-1}]
W	mean liquid flow rate [kg s^{-1}]
x	distance in the axial direction [m].

Greek symbols

δ	film thickness [m]
λ	latent heat [J kg^{-1}].

Subscripts

ave	average
f	bulk liquid
g	bulk gas
i	inlet
L	local
max	maximum
min	minimum
o	outlet
s	liquid surface.

and film inclination. Enhancement up to ~60% for the oxidation of SO_2 in a trickle bed of activated carbon catalyst in the presence of water was reported by Haure *et al.* [11] for periodic (on–off) water flow. Both symmetrical and asymmetrical flow cycling was used in that investigation, the shortest cycle period lasting 2 min. Recently, a reflux condenser was operated under steam flow pulsation in the range 0.08–0.25 Hz (Obinelo *et al.* [12]). The aim was to disperse or prevent the formation of a stable and growing condensate column above the two-phase condensing region, formed as a result of flooding in the tube. Many-fold increases in condensation capacity and heat removal rates were reported as being due to steam pulsation.

The present study is concerned with direct-contact condensation on flowing thin liquid layers covering solid substrates, e.g. packing or pipe surface. This type of condenser has received much attention in recent years, driven by water desalination equipment design and energy conversion applications, such as geothermal, solar and nuclear energy systems [13]. This work is mainly motivated by a parallel project executed in this laboratory [14] for the separation of noncondensable gases from high-pressure geothermal steam by means of a column filled with structured packing. The latter operates as a direct-contact device for the subcooled water and the geothermal gaseous stream. As steam condensation proceeds along that column, the mixture is depleted of steam and the gas stream velocity is greatly reduced, becoming very small compared to liquid film velocity. In the falling film set-up employed here, care is taken to minimize convective currents of the air–steam mixture, in order to render it effectively stagnant and to approximate conditions prevailing in part of the aforementioned direct-contact condensation column.

Experiments with a *continuous* liquid feed have already been carried out in this set-up [15–16] to determine both integral and local condensation rates. The effective resistance to condensation offered by the increased noncondensable gas concentration at the gas–liquid interface was evident in these tests. There was also strong indication of an interaction between the interfacial waves and the neighboring gas phase, implying that the *liquid* motion affected the gas phase resistance and the condensation rate. Therefore, the objective of this investigation was to explore alternative liquid flow modes that could improve direct contact condensation rates of quasi-stagnant vapor–noncondensable mixtures. For this purpose, several intermittent (periodic) liquid flow modes, of fixed 'feed' and 'pause' periods, were examined.

In the next section, mass and energy balances are solved at the mean liquid flow rate, to obtain an expression of the mean local condensation rate. The experimental set-up is briefly outlined and the results are summarized next.

COMPUTATION OF TRANSFER COEFFICIENTS

In the present problem formulation, mass and energy conservation in the moving liquid layer is employed, based on the mean liquid flow rate. In a previous paper, regarding the continuous feed operation of the same apparatus [16], an assessment was presented of three possible thermal fields within the falling liquid layer. It was ascertained that, due to the presence of relatively large amounts of noncondensables, thermal resistance to condensation resides largely in the gas phase. This implies that the amount of latent heat released by the condensing steam is almost instantly absorbed by the flowing liquid. Furthermore, turbulence and wave activity may tend to minimize all transverse temperature gradients in the film. Only a small temperature gradient associated with the thin substrate layer (a region next to the wall) was considered possible in the model developed in that study, whereas the rest of the film was assumed to have the same temperature as the interface at every axial location. Mean deviations of about 20% were calculated between predictions of that model and an

approximation involving a *flat* temperature profile throughout the liquid film.

Inasmuch as an intermittent liquid feed would be responsible for a significant turbulence level and mixing inside the liquid layer, it is reasonable to expect a rather uniform temperature ($T_f \equiv T_{ave}$) to prevail across the liquid film. Thus, mass and energy balances are made under the following assumptions:

(i) steam is everywhere saturated,
(ii) gas pressure constant at 1 atm,
(iii) the gas–liquid interface is at saturation temperature T_s,
(iv) heat losses to the surroundings are negligible,
(v) two-dimensional lateral effects are absent.

The above considerations lead to the equality, $T_{wall} = T_f = T_s$ at each cross-section along the pipe. The differential mass and energy balances over an incremental column height dx, at steady-state are:

$$dW_f = -dW_g \tag{1}$$

$$W_f Cp_f dT_f + dW_f Cp_f (T_f - T_s) + dW_g(\lambda + Cp_g(T_g - T_s)) = 0 \tag{2}$$

where W_f is the mean liquid flow rate, T_g is the average gas mixture temperature ($T_g \equiv T_{steam-air}$) and λ is the latent heat of condensation; mechanical energy terms are neglected. By combining equations (1) and (2) and integrating with respect to x, one obtains

$$m_{con} = W_{f,o} - W_{f,i} = \frac{W_{f,i} Cp_f (T_{f,o} - T_{f,i})}{\lambda + Cp_g(T_g - T_s) - Cp_f(T_{f,o} - T_s)} \tag{3}$$

where m_{con} is the condensation rate in g s^{-1}. Subscripts i and o denote inlet and outlet conditions, respectively. For a uniform temperature across the liquid film, $T_s = T_{ave}$. Hence, for every particular distance between two measuring stations the average temperatures are computed as:

$$T_s = \frac{(T_{f,o} + T_{f,i})}{2} \tag{4}$$

and

$$T_g = \frac{(T_{g,o} + T_{g,i})}{2}. \tag{5}$$

Since $T_{f,i}$, $T_{f,o}$, $T_{g,i}$, $T_{g,o}$ and $W_{f,i}$ are experimentally determined, the condensation rate m_{con} is computed from equations (3)–(5). For the interpretation of experimental data, the local heat transfer coefficient is defined as

$$h_L = \frac{\lambda}{\Delta T} \frac{m_{con}/\pi D}{\Delta x} \tag{6}$$

where Δx is the distance between two measuring stations and $\Delta T = T_g - T_{ave} = T_g - T_s$. The mean possible error in calculating h_L (at 95% confidence level) is estimated to be less than 15%. Only for cases where h_L is less than $\sim|300|$ W m^{-2} K^{-1}, the error may be much larger because small temperature differences (involving considerable relative error) are encountered in the calculations. However, such low h_L are generally of limited significance to this study.

APPARATUS AND EXPERIMENTS

The experimental set-up (Fig. 1) including measurement and data acquisition procedures are the same as those described by Karapantsios *et al.* [16]. The falling film is formed in a vertical, Plexiglass pipe of 50 mm i.d., divided in three sections, i.e. inlet (0.3 m), intermediate (0.96 m) and measurement section (1.40 m). Sufficient external pipe insulation ensures adiabatic conditions. Filtered deaerated tap water (stored in a large tank) is used in the tests, flowing only once through the system.

Steam comes from the building supply relatively free of air ($< 10^{-3}$ mass fraction air in mixture). It is released inside the pipe, at the center of the cross-section, in the direction of the liquid flow and 1.77 m below the liquid feed. A specially designed feeding section made of a perforated Teflon end-piece is used to spread the steam in the test tube, and minimize forced convection effects. The system is allowed to operate with steam at a fixed liquid rate, for almost an hour, to reach a steady state. It is then observed that steam, upon discharge to the test section, is mixed with air which appears to move downwards from the upper part of the pipe, possibly dragged by the interfacial shear exerted by the fast moving liquid. As a result, the steam–air mixture apparently moves with a finite velocity which, however, is under all circumstances relatively small (of order 10 cm s^{-1}) compared to the liquid film velocity (of order 1 m s^{-1}). Thus, for the tests reported here the gas phase may be considered effectively stagnant. Excess steam is discharged to the atmosphere through a vent located at the downstream receiving vessel.

To control the intermittent feed, the apparatus is equipped with an electropneumatic valve (G.R.I.-SAPAG, model EED.25), connected in series to the liquid by-pass line, just before the liquid entry to the flow meters. The valve is operated in an on–off mode to obtain a square-wave type of liquid feed. During the 'on' operation of the valve no liquid is fed into the vertical tube, but only some drainage is observed of liquid running over the entrance weir [17]. The valve is electrically energized by pulses of specified frequency. The time interval of pulsing is controllable separately for the 'on' and the 'off' mode by a twin timer switch (SAINT WIEN, model SW TDV), in the range 0–6 s. A high precision oscilloscope (HAMEG, model HM 205) is used to measure cycling periods. Electrical noise limits the accuracy of controlled pulses to $\sim$0.005 s. However, the response time of the mechanically moving parts of the valve, despite its improved construction, is $\sim$0.03 s and this poses a limit to cycling. Flow cycle periods of 1–2 s, under four different intermittency modes, are employed.

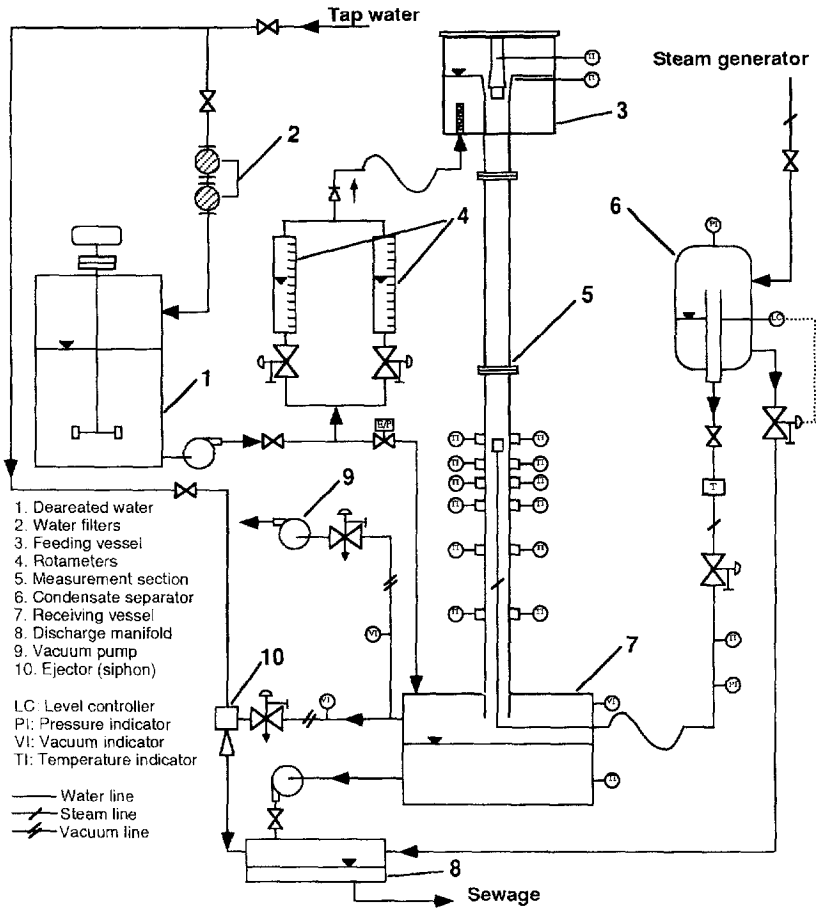

Fig. 1. Experimental set-up.

Symmetrical cycling of 1 s feed–1 s pause (**1–1**), 0.5 s feed–0.5 s pause (**0.5–0.5**), and asymmetrical cycling of 1 s feed–0.5 s pause (**1–0.5**), 0.5 s feed–1 s pause (**0.5–1**), is employed. Cycles with shorter feed periods (<0.5 s) may be adversely affected by the relatively slow mechanical response time of the electropneumatic valve. On the other hand, for longer pause periods (>1 s) it is practically impossible to maintain a continuous and uniform falling liquid layer inside the tube due to film rupture, possibly induced by surface tension effects.

Preliminary experiments were conducted to check for repeatability of the mean flow rates and to determine the number of cycles required in a run to warrant reproducible average results. A very satisfactory performance was obtained for a total number of 10 cycles in a run (data repeatability to within $\pm 2\%$). Although these checks were made for more than 10 different flow rates for each mode of intermittency, ultimately only five discrete mean flow rates were employed in this study, in the range 23–192 g s^{-1}.

Special provisions are taken to eliminate vibrations caused by the electropneumatic valve, the pumps or the flow cycling operation. Flexible tubing and connections are used to reduce hydraulic pulsations while special rubber pads and seals are employed to diminish mechanical vibrations. Nevertheless, the resonant frequency of the whole set-up is still a matter of concern. Even moderate external vibrations could be responsible for random oscillations of the test tubes with unpredictable concomittant effects in the liquid film flow. For this reason, preliminary tests were performed to determine the resonant frequency of the entire set-up. An electromagnetic vibrator (Schenck, model VIBROVID 494) was utilized to impart oscillations to the vertical test-tube by attaching its shaft to the outer tube wall, while a displacement analyser (Schenck, model VIBROPORT) was measuring the amplitude of the tube displacement. By varying the stroke frequency in the range 0.1–200 Hz, a displacement vs frequency plot was created. Details of this procedure are given elsewhere [18]. It was found that, although resonance had a peak at about 25 Hz, it was still quite appreciable in the range ~ 10 to ~ 50 Hz. This broad resonant band is typical of a dynamically unstable system, but in all cases it is well above the flow cycling frequencies employed in this study.

The temperature of the liquid film and steam–air mixture is measured at selected locations along the

measurement section of the test tube, at distances of 1.72, 1.82, 1.89, 1.99, 2.19 and 2.46 m, from the liquid entry. Considering the steam entrance level (1.77 m) as the reference ('zero') point, the aforementioned distances are designated (and referred to in the rest of this study) as −5, 5, 12, 22, 42 and 69 cm, respectively. Self-adhesive T-type thermocouples (0.0127 cm dia.), mounted on the outer surface of the Plexiglass tube in order to avoid disturbance of the liquid flow, are employed to measure the *outer* Plexiglass wall temperature. A correction (using Fourier's law) is applied afterwards to determine the *inner* pipe surface temperature. Only some qualitative tests are performed (for comparison) with miniature thermocouples slightly protruding into the liquid film. The gas mixture temperature is measured with rigid-trunk T-type thermocouples extending into the core of the pipe through appropriate ports. Using arguments presented elsewhere [16], a distance of 8–9 mm from the inner tube wall (in the radial direction) is selected as the most suitable location to measure bulk gas mixture temperature, T_g. Experiments in this work verified that at this location large liquid waves do not reach the tip of the thermocouples, as shown in Fig. 6. All thermocouples are calibrated to 0.1°C. Output signals from the self-adhesive thermocouples are sampled at 10 Hz for periods of 5–10 min. Exposed thermocouple measurements are collected in successive records, with 50 Hz sampling frequency and for periods of 100 s each.

The parallel wire, conductance probe technique [17] is used in order to measure the temporal variation of liquid film thickness. A separate probe for each measuring location is made of parallel chromel wires (diameter ~0.5 mm, length ~1 cm) spaced ~2 mm apart. Probe performance characteristics and calibration procedures are given in detail elsewhere [18] This technique is capable of resolving film thickness differences down to 0.002 mm with an overall accuracy of 0.020 mm [18]. However, only *isothermal* films are measured accurately, because otherwise as the probe wires extend inside the warmer gas phase, they attain a temperature (during condensation), higher than the actual film temperature, leading to an erroneous probe signal reference and liquid conductivity. Nevertheless, film thickness time records measured during condensation still contain useful information regarding the film variation in the time domain; i.e. frequency and streamwise velocity. Film thickness data are acquired for over 20 s periods with 400 Hz sampling frequency. Three records are taken at each flow condition to check for repeatability and to further increase the confidence of the calculated statistics. The estimated cumulative error in film thickness measurement—including calibration, measurement, digitization and data handling—is estimated to be less than 7%. The corresponding maximum possible error in calculating average wave velocities (by the cross-covariance of two simultaneous film thickness records sampled at different stations) is 18%.

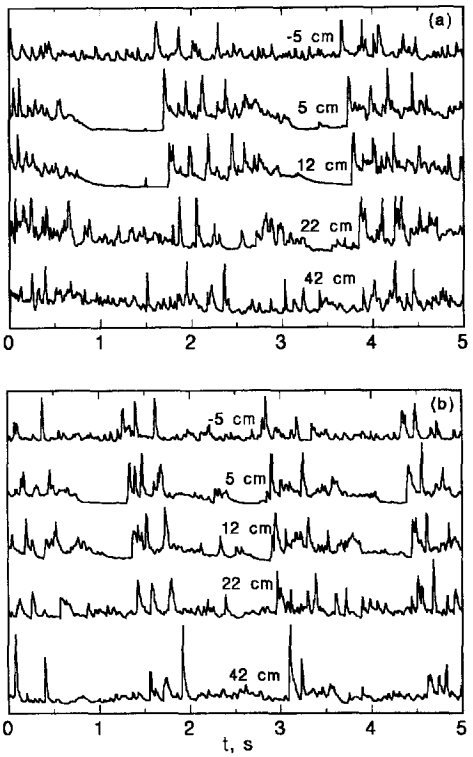

Fig. 2. Local film thickness variation during condensation at various distances from steam entry; (a) 1–1 mode, $W = 23$ g s^{-1}, (b) 0.5–1 mode, $W = 29.3$ g s^{-1}.

RESULTS AND DISCUSSION

Liquid film characteristics

Attention is focused first on film interface characteristics considered necessary for describing the hydrodynamics of the intermittent liquid layer and for explaining the condensation enhancement. Figure 2(a) displays typical traces of local film thickness *during condensation* at various distances x from steam entry, in an arbitrary ordinate scale. These time records correspond to intermittency mode 1–1 and mean inlet flow rate $W = 23$ g s^{-1}. For such a low mean flow rate and a long pause period (1 s), a film thinning effect possibly caused by thermally induced surface tension gradients is clearly evident. The intermittency mode is readily recognizable in these traces although the first one ($x = -5$ cm) corresponds to a fairly long distance (1.72 m) below liquid entry. In general, the intermittent flow pattern tends to be less pronounced in such traces at high flow rates. Additionally, the shape of the interfacial undulations does not seem to change drastically with distance and their phase velocity may be virtually constant. A similar behavior was reported by Karapantsios and Karabelas [20] for isothermal continuous flow.

Upstream of steam entry ($x = -5$ cm), the interfacial characteristics are very similar to those of the isothermal film, since the subcooled liquid film exhibits only a very small temperature rise up to this location. At tube locations (e.g. $x < 12$ cm) where

the gas mixture temperature is elevated (hot regions), surface tension effects may come drastically into play. During the feed part of the flow cycle, large lumps of liquid moving over a thin substrate, roll down with an appreciable velocity and have a relatively short residence time within the hot regions. On the other hand, in-between successive large lumps, the thin substrate flows slowly downwards, exposed to the hot regions for longer periods. This difference in exposure times may be responsible for an unequal heating of the liquid film during the flow cycle. This effect may create significant surface tension gradients within the hot regions which might be capable of pulling liquid away from the hotter thin substrate towards the large lumps of liquid [see trace at $x = 5$, 12 cm in Fig. 2(a)]. The situation is relaxed further downstream where inertial forces overcome surface tension forces, the latter already reduced due to thermal equalization within the film.

A situation similar to that of Fig. 2(a) is observed for the intermittency mode 0.5–0.5 but not presented here due to space limitations. Interestingly, for the intermittency mode 0.5–1 [Fig. 2(b); $W = 29.3$ g s^{-1}] the situation is quite different. The substrate regions appear to be shorter (<1.0 s) than expected, suggesting that the substantially larger and faster waves of this mode (quantitatively characterized below) override and partially spread over the substrate. Such large and fast moving waves may be capable of overcoming surface tension gradients and of creating vigorous agitation within the liquid film and in the neighboring gas boundary layer. On the contrary, the waves corresponding to intermittent flow 1–0.5 are the smallest and slowest compared to those of all other modes, at the same mean flow rate.

Useful insights are gained by examining the statistical characteristics of the falling liquid layer. The hydrodynamics of such isothermal free-falling films have already been investigated in this laboratory (17, 24), in a similar vertical flow loop for the case of *continuous* operation. Extensive experiments were conducted in the present study to determine the characteristics of the *isothermal* falling film for the different modes of flow intermittency. Additional data on isothermal film characteristics and continuous flow were also obtained [20]. Various quantities of the film thickness records, $\delta(t)$, were calculated assuming that $\delta(t)$ is stationary and ergodic in nature [21]. Specifically, the mean, δ_{mean}, the standard deviation, s, the maximum, δ_{max}, and the minimum, δ_{min}, were computed. The average streamwise wave velocity and frequency were also obtained on the basis of the cross-covariance, and spectral density function [21].

To calculate the above quantities from the measurements, a 8192-point sample was used, obtained with a sampling frequency of 400 Hz. The average streamwise velocity, V_{wave}, was estimated by dividing the distance between two measuring stations by the time delay corresponding to the cross-covariance peak of the respective film thickness records. Dominant

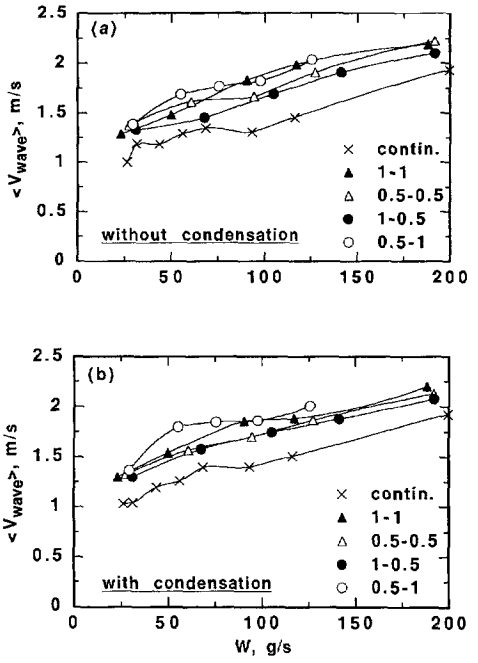

Fig. 3. Variation of average wave velocity, V_{wave}, with mean liquid flow rate; (a) without condensation; (b) with condensation.

frequencies were determined from the spectra which were calculated, with a method employed by Karapantsios *et al.* [17], using data set segmentation into groups of 512 points and final smoothing in the frequency domain.

All statistical parameters for the isothermal film plotted against longitudinal distance are given elsewhere [18]. Interestingly, in almost all cases these quantities (δ_{mean}, s, δ_{max} and δ_{min}) seem to vary randomly about an average value with no clear dependence on axial location. Only some wave velocity data exhibit a small variation with axial distance under both isothermal and condensation conditions. This behavior is somewhat different compared to the slight longitudinal variation of *all* these quantities for a continuous flow operation [20]. In order to facilitate the comparison between intermittent and continuous flow measurements, it was decided to employ space-averaged data (denoted by $\langle\rangle$) over all measuring stations. Figure 3(a) and (b), presents the average streamwise wave velocity, $\langle V_{wave}\rangle$, obtained without and with condensation, respectively. A striking similarity exists between the two cases, regardless of flow mode. Interestingly, the slope of the continuous flow experiments is practically the same as the slopes of the various intermittency modes. This may imply that, with increasing liquid flow rate, the same mechanism(s) influence the wave growth and motion irrespective of feeding modes. However, it will also be pointed out that the wave velocities for intermittent feed are systematically greater, compared to continuous liquid feed, and that overall the mode 0.5–1 exhibits the highest velocities.

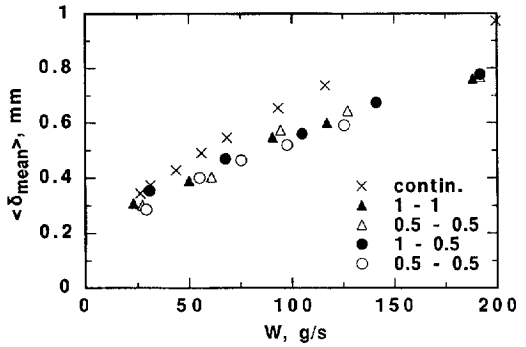

Fig. 4. Variation of average film thickness, $\langle \delta_{mean} \rangle$, with mean liquid flow rate.

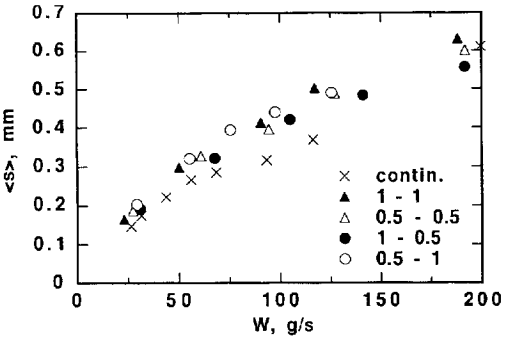

Fig. 5. Variation of standard deviation, $\langle s \rangle$, with mean liquid flow rate.

From the numerous spectra calculated in this work (not presented here)—both with and without condensation—it was not possible within the experimental uncertainty to detect any systematic longitudinal variation of the characteristic frequency. The same observation was also made in experiments carried out under continuous flow conditions [16]. In general, spectra from condensation experiments resemble those of the isothermal flow but exhibit somewhat broader peaks. All these observations, in connection with the streamwise wave velocities and dominant frequencies, suggest that the interfacial structure is not altered significantly by condensation, at least inasmuch as the large waves are concerned. These large waves not only cover most of the film surface area, but also carry the major part of the liquid flow. Therefore, it seems reasonable to investigate the characteristics of the *isothermal* film and then extend the conclusions to the case of condensation. It will be recalled that, due to the constraints posed by the experimental technique employed for measuring film thickness, it is not possible to obtain directly records of the film thickness variations during condensation.

Figure 4 displays the temporal and spatial mean film thickness vs the mean inlet liquid flow rate. All intermittency modes appear to have $\langle \delta_{mean} \rangle$ values close to each other, falling below the continuous flow data. With increasing W this difference between continuous and intermittent modes tends to increase, while at very low W it almost disappears. This indicates that the effects of the particular feed cycling examined in this study may be more pronounced at higher liquid flow rates. The reduction of mean film thickness associated with intermittent feed is consistent with available experimental evidence in the literature [20, 22, 23], showing that fast moving waves tend to reduce the mean thickness. In Fig. 5 the standard deviation $\langle s \rangle$ is plotted against W. This quantity provides a measure of the 'dispersion' of data about their mean value. It is seen that, for $W < \sim 70$ g s^{-1}, intermittency is responsible only for a minor increase in $\langle s \rangle$ while, for larger W, the increase is appreciable, with the exception of a point at ~ 200 g s^{-1}.

Figure 6 presents the variation of $\langle \delta_{max} \rangle$ with W.

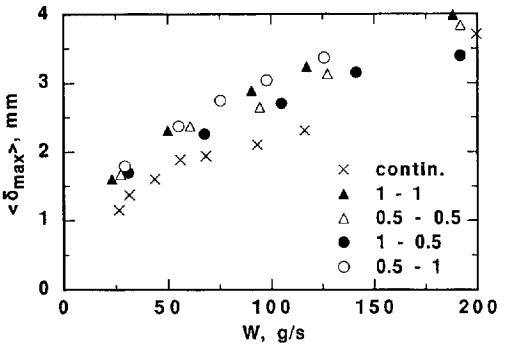

Fig. 6. Variation of maximum film thickness, $\langle \delta_{max} \rangle$, with mean liquid flow rate.

The same general trends identified in Fig. 5 also hold here. Again, at $W \sim 200$ g s^{-1}, there is practically no difference between the data. This is interesting inasmuch as distinct larger lumps of liquid might be expected for the intermittent flow as compared to the continuous flow. Thus, it seems that at W ~ 200 g s^{-1} (corresponding to an isothermal film Reynolds number ~ 5200) wave growth has reached an upper limit. This suggestion is in agreement with an observation made in previous papers [17, 24], i.e. that at $Re \sim 5000$ the amplification of large waves seems to stop and a gradual amplification of ripples and smaller waves on the substrate takes place.

The variation of $\langle \delta_{min} \rangle$ vs mean liquid flow rate is plotted in Fig. 7. These minimum values reflect the thin substrate film in the intermediate period between large lumps of liquid, created when no liquid is fed into the test-tube at the 'pause'. Consequently, it is not surprising that $\langle \delta_{min} \rangle$ increases only slightly with W for all modes of intermittency. On the other hand, the substrate minimum thickness during the continuous operation increases significantly with W.

Condensation heat transfer coefficients

The bulk steam–air and inner wall (liquid) temperatures are plotted against longitudinal distance in Fig. 8. Owing to space limitations only the data for the 0.5–0.5 intermittency mode are presented here. Similar graphs for the other modes are included in a

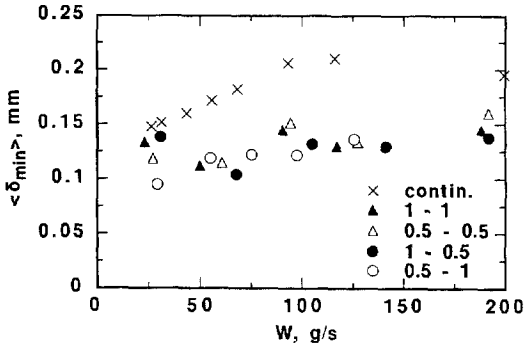

Fig. 7. Variation of minimum film thickness, $\langle \delta_{min} \rangle$, with mean liquid flow rate.

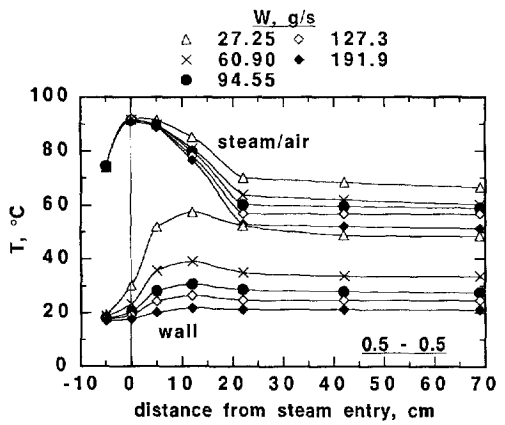

Fig. 8. Variation of $T_{steam-air}$ and T_{wall} with longitudinal distance.

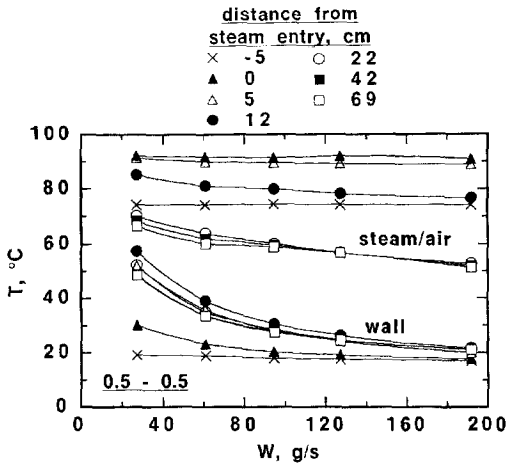

Fig. 9. Variation of $T_{steam-air}$ and T_{wall} with mean liquid flow rate.

thesis by one of the authors [18]. Moreover, the trends and the general characteristics of the curves are very similar for the various modes so that the behavior depicted in Fig. 8 is quite representative of all modes.

The gas mixture temperatures are at a maximum near the steam exit point. The relatively high temperature upstream of that point (at $x = -5$ cm) is due to steam escaping upwards from the steam entry. This proved inevitable despite efforts made to reduce the available gas space at the steam entry by the (cylindrical) steam distributor Teflon-piece. For axial distances smaller than 22 cm $T_{steam-air}$ falls off sharply, while for greater distances it drops only gradually. It is noted that these temperatures correspond to saturation conditions so that steam mole fractions can be directly estimated from these measurements. For the data presented in Fig. 8, steam mole fractions vary between ~ 0.15 and ~ 0.75. As for the variation of T_{wall} with distance, it reaches a maximum at approximately 12 cm below steam entrance and then drops gradually. This behavior possibly indicates that the liquid surface at this distance has exceeded the interfacial saturation temperature on the gas side (in all cases lower than the corresponding bulk gas saturation temperature) so that the adverse evaporation phenomena start. For the continuous feed operation [16], this 'inversion' is observed only at low liquid flow rates ($< \sim 50$ g s^{-1}).

Figure 9 presents the variation of $T_{steam-air}$ and T_{wall} vs the mean inlet liquid flow rate. For distances less than 5 cm, above and below steam entry, $T_{steam-air}$ is practically constant throughout all W, but for further downstream locations it gradually drops. On the other hand, a rather drastic reduction of T_{wall} with W is observed. Interestingly, for locations greater than 5 cm, all curves have almost the same slope, at all liquid flow rates. Similar trends to those observed in Figs. 8 and 9 are also reported for the continuous flow operation of the same apparatus [16]. It is clear from Figs. 8 and 9 that the most important part of the tube length, with respect to condensation, corresponds to the first few centimeters (above and) below steam entry.

In Fig. 10(a)–(d) the local condensation heat transfer coefficients for all intermittency modes are plotted against mean inlet liquid flow rate. The coefficients determined from the continuous flow experiments are also included in the plots for comparison. An inspection of Fig. 10(a) and (b) reveals that, for locations close to the steam entrance, surprisingly high coefficients are obtained for all intermittency modes as compared to continuous flow. In some cases, an increase of almost an order of magnitude is observed. Interestingly, in the section 0–5 cm [Fig. 10(b)], *where a major part of the overall condensation takes place*, the 0.5–1 mode yields the highest heat transfer coefficients. It may be recalled here that at this particular flow mode the largest and fastest liquid waves [as shown in Figs. 2(b) and 3(b)] travel along the test tube. This may offer a plausible interpretation for the relatively large condensation rates measured with the intermittency mode 0.5–1. At the lowest flow rates (~ 25 g s^{-1}) the h_L values are almost identical for all intermittency modes except the 1–0.5 one, where the heat transfer enhancement is found to be less pronounced. This particular asymmetrical flow rate,

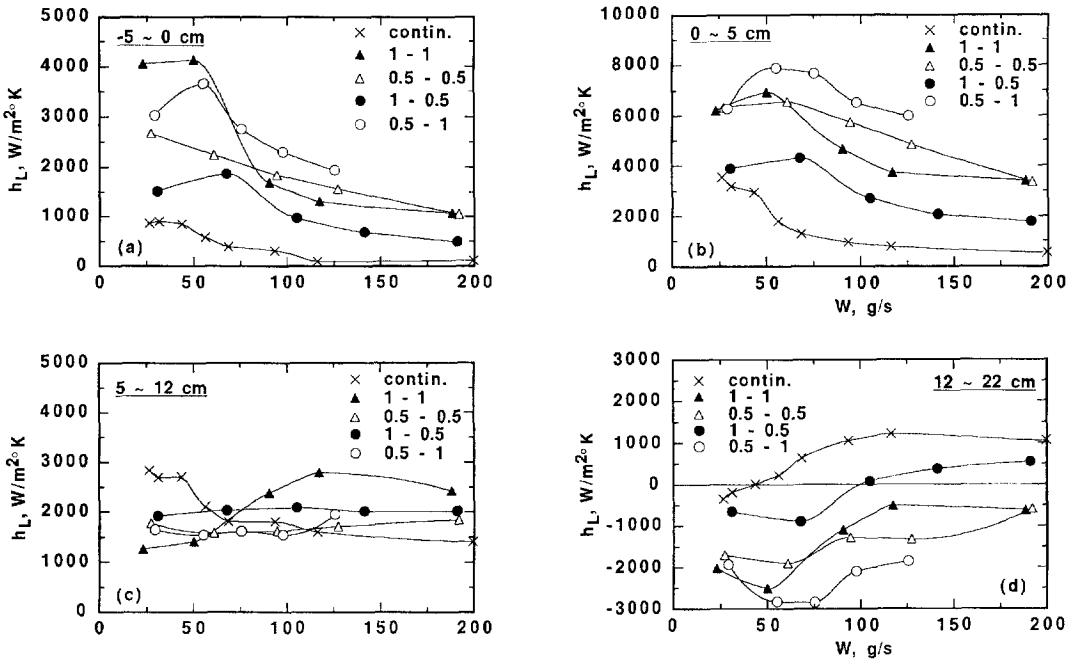

Fig. 10. Local condensation heat transfer coefficient, h_L, vs mean liquid flow rate at various longitudinal locations.

resembles *more* the continuous liquid flow in that only one third of the cycle period is without liquid feed. On the contrary, the asymmetrical mode 0.5–1 is the one differing most from the continuous flow case. The two symmetrical intermittency modes give coefficients in close proximity, a behavior which is generally observed in the rest of the plots; i.e. Fig. 10(c) and (d). Thus, it seems that (over the range of periods studied) the system performance does not depend so much on the frequency of flow pulsation but rather on the symmetry of the intermittency, or lack thereof. Additionally, with respect to Fig. 10(a) and (b), it may be argued that the possibly more intense flow fluctuations accompanying the 0.5–0.5 mode, relative to the 1–1 mode, may be responsible for the slightly greater coefficients of the former at high flow rates. In general, it appears that performance improvement by flow cycling is less pronounced at low liquid flow rates, where, even with the continuous mode, relatively high condensation coefficients are achieved.

Upon inspection of Fig. 10(c) and (d) it is seen that for the continuous flow operation (at distances greater than 12 cm) condensation still takes place for most of the flow rates, while for the intermittent operation, some evaporation phenomena are also observed. Interestingly, in terms of efficiency, the evaporation heat transfer coefficients at the different flow modes are in the same order as the condensation coefficients; that is, the 0.5–1 mode is again more effective. This implies that similar physical mechanisms may dominate the transport process in both phenomena. Another point of interest is the variation of h_L with W. When intense condensation phenomena prevail [in regions with high steam concentration, Fig. 10(a) and (b)], h_L decreases with W, but levels off a little further downstream [Fig. 10(c)], where mild condensation rates are involved. However, for longer longitudinal distances [> 12 cm; i.e. Fig. 10(d)] where only limited condensation takes place, the major transport process being evaporation, h_L is an increasing function of W. This behavior holds for all flow modes and may be related to the local flow pattern developing on the gas side by the interaction with the liquid surface undulations [18].

The trends observed in Fig. 10 are here reexamined on the basis of equation (6). Thus, increased heat transfer rates during flow cycling may be attributed either to an increased condensation rate m_{con}, or to a reduced thermal driving force, $\Delta T = T_g - T_s$. It will be recalled that $T_s \equiv T_{wall} \equiv T_{ave}$. Figure 11(a)–(c) contrasts the thermal driving force for the intermittent and continuous flow operation, for three segments of the test section. Similar graphs are obtained for other (downstream) tube segments. It is shown that, although $T_g - T_s$ for the continuous case is almost always higher (by 10–20%), that difference alone cannot account for the much larger coefficients determined during flow cycling [Fig. 10(a) and (b)]. Generally, it appears that the trends depicted in Fig. 10(a)–(d) cannot be inferred solely from the trends in Fig. 11(a)–(c). A plausible explanation for the present condensation enhancement may be obtained by using arguments that have been previously advanced [16] for the continuous flow operation. Indeed, condensation enhancement may be the result of a possible interaction between interfacial waviness and the

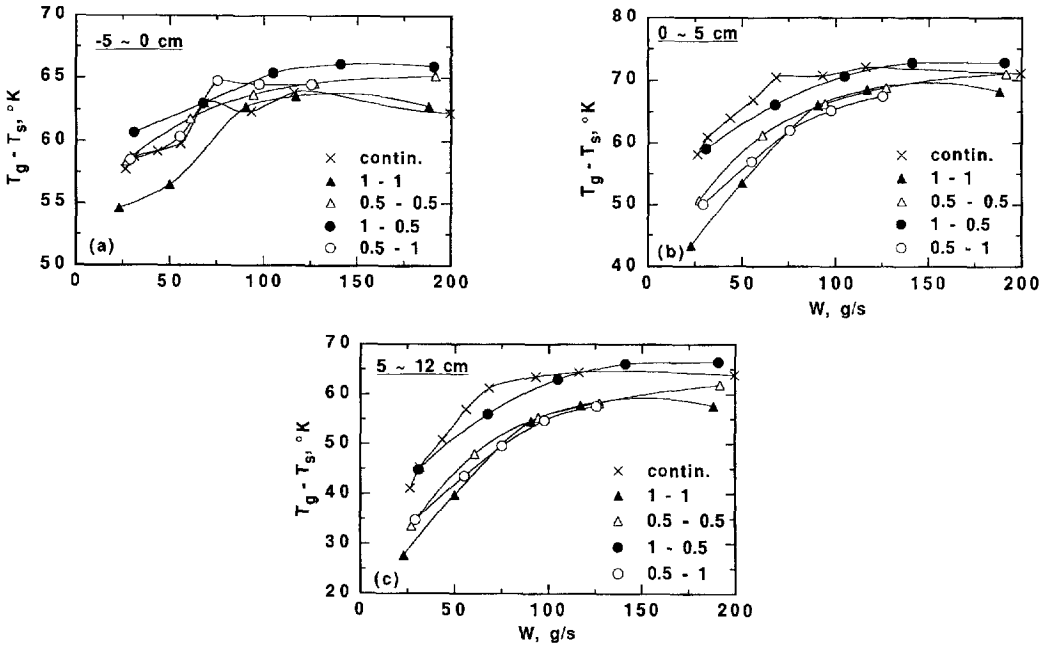

Fig. 11. Local thermal driving force, $\Delta T = T_g - T_s$, vs mean liquid flow rate at various longitudinal locations.

apparent mass boundary layer at the gas side insofar as the liquid side thermal resistance is negligible. This gas boundary layer is due to the buildup of non-condensable gas near the interface through which the vapor must diffuse to reach the subcooled liquid film [1]. Flow intermittency probably induces significant shear to the gas phase which results in small scale local agitation of the mass transfer boundary layer on the gas side, with the ultimate effect of reducing its effective thickness.

CONCLUDING REMARKS

Local condensation heat transfer coefficients, h_L, are greatly dependent both on liquid feeding mode and liquid flow rate. Flow intermittency, in general, may enhance the transport process by even an order of magnitude, in terms of condensation rates. This is interesting because in the present experimental set-up the major thermal resistance resides in the *gas* side. Thus, liquid flow cycling affects not only the liquid flow characteristics but also gas phase conditions at the interface. As the literature lacks sufficient evidence on this issue, the significance of the present work is not only confined to this direct-contact condensation experiment. It is further shown that, for the frequency range employed in this study, cycling frequency has only a minor effect on condensation. What seems to be more important is the asymmetry of intermittency. A flow cycle mode with a short feed period (0.5 s) and a long pause period (1 s) gives the highest transfer rates.

In an attempt to investigate the relationship between heat transfer enhancement and interfacial morphology of the falling liquid layer, several statistical quantities of the film thickness are calculated. Measurement of the film thickness fluctuations show that the periodic changes in flow characteristics, imposed at the liquid entry, retain their form and shape to a considerable extent much further downstream (> 1.70 m). Experimental evidence on the average wave velocity and dominant frequency range, both with and without condensation, reveals that the interface is not drastically modified by the condensing vapor. It appears that large roll waves remain practically unaffected and only minor surface disturbances may be significantly damped during condensation. For a fixed mean liquid flow rate, the wave velocity, film thickness standard deviation and maximum values are higher for the intermittent feed as compared to the continuous flow operation; on the contrary the mean and the minimum film thickness are lower.

In conclusion, it appears that augmentation of interfacial transport is linked to the surface characteristics of the falling liquid film. In particular, it seems that the higher transport rates correspond to the flow mode with the largest and fastest waves, at a given mean flow rate. Thus, efforts must be headed towards shorter feed and/or larger pause periods. However, in this study, larger pause periods are excluded due to the film rupture effect which is undesirable, whereas implementation of shorter feed periods is hindered by mechanical problems.

Acknowledgements—This work has been supported in part by the Commission of European Communities (under programme VALOREN and contract JOU2-CT92-0067). Helpful discussions with Dr V. Bontozoglou are greatly appreciated.

REFERENCES

1. J. G. Collier, *Convective Boiling and Condensation*. McGraw-Hill, London (1972)
2. A. G. Williams, S. S. Nandapurkar and F. A. Holland, A review of methods for enhancing heat transfer rates in surface condencers, *Chem. Engr* CE 376–373 (1968).
3. J. A. Shmerler and I. Mudawar, Local evaporative heat transfer coefficient in turbulent free-falling liquid films, *Int. J. Heat Mass Transfer* **31,** 731–742 (1988).
4. D. R. Oliver and T. E. Atherinos, Mass transfer to liquid films on an inclined plane, *Chem. Engng Sci.* **23,** 525–536 (1968).
5. N. Brauner and D. M. Maron, Characteristics of inclined thin films, waviness and the associated mass transfer, *Int. J. Heat Mass Transfer* **25,** 99–110 (1982).
6. A. E. Dukler, The role of waves in two-phase flow: some new understanding, *Chem. Engng Educ.* (Award Lecture) 108–138 (1977).
7. M. J. McCready and T. J. Hanratty, Effect of air shear on gas absorption by a liquid film, *A.I.Ch.E. Jl* **31,** 2066–2074 (1985).
8. K. Muenz and J. M. Marchello, Surface motion and gas absorption, *A.I.Ch.E. Jl* **12,** 249–253 (1966).
9. S. L. Goren and R. V. S. Mani, Mass transfer through horizontal liquid films in wavy motion, *A.I.Ch.E. Jl* **14,** 57–61 (1968).
10. N. Brauner and D. M. Maron, Mass transfer in inclined thin films with intermittent feed, *Chem. Engng J.* **26,** 105–117 (1983).
11. P. M. Haure, R. R. Hudgins and P. L. Silveston, Periodic operation of a trickle-bed reactor, *A.I.Ch.E. Jl* **35,** 1437–1444 (1989).
12. I. F. Obinelo, G. F. Round and J. S. Chang, Condensation enhancement by steam pulsation in a reflux condenser. In *Experimental Heat Transfer, Fluid Mechanics and Thermodynamics* (Edited by J. F. Keffer, R. K. Shah and E. N. Ganic). Elsevier, New York (1991).
13. F. Kreith and R. F. Boehm (Eds), *Direct-contact Heat Transfer*. Hemisphere, New York (1988).
14. V. Bontozoglou and A. J. Karabelas, Simultaneous direct-contact condensation and noncondensable gas absorption in columns with structured packing, *A.I.Ch.E. Jl* (1995).
15. T. D. Karapantsios, M. Kostoglou and A. J. Karabelas, Direct contact condensation of steam on wavy falling films, Paper D4, 29*th Meeting of the European Two-phase Flow Group*, Stockholm, 1–3 June (1992).
16. T. D. Karapantsios, M. Kostoglou and A. J. Karabelas, Local condensation rates of steam–air mixtures in direct contact with a falling liquid film, *Int. J. Heat Mass Transfer* **38,** 779–794 (1995).
17. T. D. Karapantsios, S. V. Paras and A. J. Karabelas, Statistical characteristics of free falling films at high Reynolds numbers, *Int. J. Multiphase Flow* **15,** 1–21 (1989).
18. T. D. Karapantsios, Flow of a thin liquid film in a vertical pipe. Direct-contact condensation phenomena, Doctoral Dissertation (in Greek), Department of Chemical Engineering, University of Thessaloniki (1994).
20. T. D. Karapantsios and A. J. Karabelas, Longitudinal characteristics of wavy falling films, *Int. J. Multiphase Flow* **21,** 119–127 (1995).
21. J. S. Bendat and A. G. Piersol, *Random Data: Analysis and Measurement Procedures*. John Wiley, New York (1986).
22. H. Takahama and S. Kato, Longitudinal flow characteristics of vertically falling liquid films without concurrent gas flow, *Int. J. Multiphase Flow* **6,** 203–215 (1980).
23. G. J. Zabaras, Studies of vertical annular gas–liquid flows, Ph.D. Thesis, University of Houston (1985).
24. T. D. Karapantsios and A. J. Karabelas, Surface characteristics of roll waves on free falling films, *Int. J. Multiphase Flow* **16,** 835–852 (1990).